Structural Characterization, DFT Calculations, Metal Uptake, Fluorescence, Antimicrobial and Molecular Docking Studies of Novel Co(II) and Ni(II) Complexes with NNS Tridentate Schiff base Ligand

omyma ali (omaymaahmed92@yahoo.com)
Ain Shams University https://orcid.org/0000-0002-3240-1250
Doaa A. Nassar
Ain Shams University, Cairo
Mohamed R. Shehata
Cairo University
Abeer S.S. Sayed
Ain Shams University, Cairo

Research Article

Keywords:

Posted Date: January 25th, 2022

DOI: https://doi.org/10.21203/rs.3.rs-1277441/v1

Abstract

A new Schiff base ligand N^2-((5-methylthiophen-2-yl) methylene) pyridine-2,6-diamine (L) was prepared by condensation of 5-Methyl-2-thiophenecarboxaldehyde and 2,6-diaminopyridine in ethanol in a molar ratio 1:1. The ligand and its complexes were characterized based on elemental analyses, molar conductance, magnetic moment, IR, MS, ^{1}H NMR, solid reflectance, and thermal analysis (TG and DTG) techniques. The complexes were found to have the formulas $[CoL(H_2O)\ Cl_2].H_2O$ and $[NiL(H_2O)Cl_2].2H_2O$. From FTIR spectral data, the coordination between the ligand L to the central metal ion was through its nitrogen of pyridyl and azomethine and sulfur of 2-thiophenecarboxaldehyde. The metal complexes were found to be nonelectrolyte. Octahedral geometries of the Co(II) and Ni(II) complexes were investigated from electronic and magnetic data. The kinetic analysis of the thermogravimetric data was performed by using the Coats-Redfern equation. The fluorescence properties of the ligand and its complexes in DMF were studied. The values of optical band gap energy (Eg) of the synthesized complexes suggested that these compounds could be used as semiconductors. The adsorption of Co^{2+} and Ni^{2+} in aqueous solutions on ligand under various conditions was studied. The maximum adsorption percentage of Co(II) and Ni(II) were found to be 68% and 65%, respectively. The Molecular docking studies were executed to consider the nature of binding and binding affinity of the synthesized compounds with the receptor of Bacillus subtilis (gram +ve bacteria) and Escherichia coli (gram –ve bacteria) (PDB ID: 1fj4). The ligand and its complexes were tested as antimicrobial agents.

1. Introduction

Transition metal complexes with nitrogen, sulphur, or oxygen as ligand atoms were becoming more important because these Schiff bases can bind with various metal centers involving various coordination sites, allowing for the successful synthesis of metallic complexes with interesting stereochemistry [1, 2]. Moreover, Sulphur and nitrogen-containing ligands and their transition metal complexes were employed as corrosion inhibitors [3, 4], extreme pressure lubricant additives [5] and showed broad biological activity [6–10] due to the different ways in which they were bonded to metal ions. Heterocyclic compounds such as pyridine, 2,6-diaminopyridine, and related molecules are good ligands because of the presence of at least one ring nitrogen atom with a localized pair of electrons [11, 12]. Heterocyclic compounds were the most abundant in nature and were required for a wide range of applications in biology including antibacterial, antifungal, anticancer, antioxidant, anti-inflammatory activity, and also in analytical processes [13–17]. These heterocycle-containing compounds have important properties in the fields of material science and biological systems [18, 19].

In the present study, we reported the synthesis and characterization of a novel Schiff base derived from the condensation of 5-Methyl-2-thiophenecarboxaldehyde and 2,6-diaminopyridine, and its complexes with Co(II) and Ni(II). There were many spectroscopic tools utilized to characterize the synthesis complexes elemental analysis, molar conductivity, ^{1}H NMR, IR and solid reflectance, magnetic moment, thermal analyses (TG/DTG), and fluorescence spectra studies.

2. Experimental

2.1 Materials and reagents

5-Methyl-2-thiophenecarboxaldehyde, 2,6-diaminopyridine and the metal salts; $CoCl_2.6H_2O$ and $NiCl_2.6H_2O$ were brought from sigma Aldrich company. All solvents were of analytical reagent grade (AR) and had the highest purity available. They were used without further purification.

2.2 Instrumentation

The elemental analysis of ligand and its metal complexes was performed using Perkin– Elmer CHN 2400. The molar conductivity of freshly prepared DMF solutions (1 x 10^{-3} M) at 25 ºC was measured for the dissolved complexes using Jenway 4010 conductivity meter. The infrared spectra with KBr discs were recorded using a Perkin-Elmer spectrophotometer model 1430, in the range 400-4000 cm^{-1}. ^1H NMR spectra were obtained on a Bruker AMX 500 spectrometer at 500.13 MHz in the $CDCl_3$ solution with TMS as an internal reference. The melting points were measured at Electrothermal 9200. Mass spectrometry of the solid ligand was measured on a JEOL JMS-AX 500 spectrometer. Magnetic susceptibility measurements were carried out using the Gouy method on a Sherwood magnetic susceptibility balance at room temperature. A Shimadzu 3101 pc spectrophotometer was used to calculate solid reflectance spectra. The photoluminescent properties of all the compounds were studied using an LS50B Jenway 6270 Fluorimeter. The thermal studies TG/DTG–50H were carried out under a nitrogen atmosphere with a heating rate of 10 ºC/min. using a Shimadzu DT-50 thermal analyzer.

2.3 Synthesis of the Schiff base ligand N^2-((5-methylthiophen-2-yl) methylene) pyridine-2,6-diamine (L)

The Schiff base, L ligand was synthesized by adding the ethanolic solution of 5-Methyl-2- thiophenecarboxaldehyde (1.13 g, 9 mmol) with a solution of 2,6-diaminopyridine (0.98 g, 9 mmol) in hot ethanol and stirring for 8 hours. The color of the reaction mixture was changed from pale yellow to brown color with the formation of the precipitate. The isolated brown Schiff base was washed several times with diethyl ether and dried in a vacuum.

2.4 Preparation of the metal complexes

A general procedure was employed for the synthesis of the reported complexes by adding equimolar amounts of a methanolic solution of the selected metal salts to THF solution of Schiff base L ligand in the molar ratio 1:1. The reaction mixtures were heated to reflux for 6 hours. The resulting solution was concentrated by evaporation and the precipitate was then isolated, washed with hot petroleum ether several times and then the complex was left to dry in vacuo for several hours. Table 1 gave the reaction period, the color of complex and % yield.

Table 1
Physical data and analytical of the Schiff base ligand (L) and its metal complexes

Compound	M.Wt.	Color	Yield %	M.P. ºC	Molar conductance ($\Omega^{-1}mol^{-1}$ cm^2)(*)	Elemental analysis Found (calc.)			
						C%	N%	H%	S%
L ($C_{11}H_{11}N_3S$)	(217.28)	brown	88	250	-	60.89 (60.80)	19.03 (19.33)	12.37 (12.10)	14.75 (14.76)
[Co($C_{11}H_{11}N_3S$)(H_2O)Cl_2].H_2O	(383.13)	Brownish green	70	>300	27	34.84 (34.48)	10.78 (10.6)	3.04 (3.94)	8.18 (8.37)
[Ni($C_{11}H_{11}N_3S$)(H_2O)Cl_2].$2H_2O$	(400.9)	Dark brown	78	>300	16	32.54 (32.95)	10.65 (10.48)	4.03 (4.27)	7.65 (7.99)
(*) Solutions in DMF (10^{-3} M).									

2.5 Metal ion uptake study

The metal ion uptake study was done by batch technique. A batch experiment was carried out to investigate the adsorption of Co(II) and Ni(II) ions using ligand L. The adsorption tests were performed by introducing 5 mg ligand in a

flask containing 10 mL of the prepared aqueous solution of each of $CoCl_2.6H_2O$ and $NiCl_2.6H_2O$ (0.01M, 0.001M and 0.0001M) in a flask at room temperature and filtered after different times 1, 2 and 5 hours. Then, the supernatant was filtered and the concentration of the residual metal was determined complexometrically by titration against a standard solution of EDTA-Na using the suitable indicator at a suitable pH value [20]. The removal percentage % of metal was calculated using the following equation:

$$\text{Removal \%} = \frac{C_o - C_e}{C_e}$$

Where:

C_o is the initial concentration of metal ions (mg/L).

C_e is the concentration of metal ions at time t (mg/L).

2.6 DFT calculations

Density functional theory (DFT) for geometry optimization and frontier molecular orbitals were calculated for the ligand and its complexes. B3LYP functional was employed with a 6-311G++(d,p) basis set for C, H, N, O, S and Cl and LANL2DZ for cobalt and nickel in the gas phase [21]. All calculations were performed by using the Gaussian 09 program package [22].

2.7 Microbiological investigation

The synthesized metal complexes were screened for antibacterial activity against two local Gram-positive bacterial species (*Streptococcus pneumonia* and *Bacillus subtilis*) and two local Gram-negative bacterial (*proteus vulgaris* and *Escherichia coli*) on nutrient agar medium (NA). Also, the antifungal activities were tested against two local fungal species (*Aspergillus fumigatus* and *Candida albicans*) on Sabouraud Dextrose Agar (SDA) medium. Gentamycin and Ketoconazole were used as standard references for Gram-positive & Gram-negative bacteria and fungi, respectively served as positive controls. In the agar, well diffusion method, the wells (6 mm in diameter) were dug in the media with the help of a sterile borer with centers at least 24 mm apart [23]. The concentration of the test samples (1 mg/ml in DMF) was introduced in the respective wells. The plates were then incubated at 37 ºC and 25 ºC for bacteria and fungi, respectively.

Generally, the antimicrobial agent diffuses in the agar medium and inhibits the germination and growth of the test microorganism and then the diameters of inhibition growth zones were measured in millimeters, after 24 h for bacteria and 48 h for fungi as an indicator for antimicrobial activity and the obtained results are represented as no activity, low activity, intermediate activity and high activity. The assay was carried out in triplicate. The zone diameters values were averaged and the mean values were tabulated.

2.8 Molecular docking

Molecular docking studies were achieved with MOA2019 software [24], to find out the possible binding modes of the ligand and the complexes with the receptor of gram –ve bacteria (Escherichia coli) (PDB ID: 1fj4) [25] and gram +ve bacteria (Bacillus subtilis) (PDB ID: 1QD9) [26]. The optimized structure of ligand and complexes from the output of Gaussian09 calculations were created in PDB file format. The crystal structures of the receptors were downloaded from the protein data bank (http://www.rcsb.org/pdb).

3. Results And Discussion

In this work, The Schiff base ligand N^2-((5-methylthiophen-2-yl) methylene) pyridine-2,6-diamine and its Co(II) and Ni(II) complexes were synthesized and characterized by several analytical and spectroscopic techniques. Several attempts to create single crystals of complexes suitable for crystal analysis failed due to their poor solubility in common organic solvents. Elemental analyses and some physical properties of the ligand and its complexes were listed in Table 1.

3.1 Elemental analysis and physical properties

The analytical & physical data of the Schiff base ligand (L) and its metal(II) complexes were supported the proposed structure for all compounds as 1:1 metal to ligand stoichiometry (Table 1). The presence of hydrated/ coordination water molecules was supported by TG/DTG analysis. Additionally, all the resulting complexes were colored, stable at room temperature, non-hygroscopic, and insoluble in the most common organic solvents.

3.2 Conductivity and magnetic measurements

The molar conductivities of Co(II) and Ni(II) complexes were measured in DMF (10^{-3} M) as shown in Table 1. The observed values for Co(II) and Ni(II) complexes showed non-electrolyte natural. The observed magnetic moment values for Co(II) and Ni(II) complexes were found to be 4.6 and 3.85 B.M., respectively [27, 28]. These values suggested a coordination number of six for the central metal ions and an octahedral geometry [27, 29].

3.3 IR spectra studies

The IR spectra of the Co(II) and Ni(II) complexes were compared with those of the free ligand to determine the involvement of coordination sites in chelation (Table 2).

Table 2
Most important IR spectral bands of the ligand (L) and its metal complexes.

Compound	IR spectra (cm^{-1})[a]				
	$\upsilon(NH_2)$ or $\upsilon(H_2O)$	υ(C=N)	δ(py)	υ (M-N)	υ(M- S)
L	3464(m), 3386(m)	1613(s)	626(w)	-	-
$[CoL(H_2O)Cl_2].H_2O$	3379(b)	1644(b, m)	631(w)	532(w)	468(w)
$[NiL(H_2O)Cl_2].2H_2O$	3376(b)	1630(b,m)	630(w)	530(w)	457(w)
[a] s, strong; w, weak; b, broad; m, medium					

The IR spectrum of the Schiff base ligand (Fig. 1) showed the appearance of two bands at 3464 and 3386 cm^{-1} which may be assigned to $v_{as}(NH_2)$ and $v_s(NH_2)$ [30]. The IR spectra for Co(II) and Ni(II) complexes exhibited broad band at 3379 and 3376 cm^{-1}, respectively assigned to v(OH) of crystalline or coordinated water molecules associated with the complex. This band may be overlapped with the band corresponding to the stretching vibration of $v(NH_2)$ group [31]. The IR spectrum of the ligand exhibits a band at 1613 cm^{-1} due to v(C=N) of the azomethine group [32]. After complexation, the peak assigned to v(C=N) was moved to a higher region by about 17-31 cm^{-1} suggesting coordination through N atom of the azomethine group [33]. Also, the in-plane deformation band of pyridine was observed for Schiff base at 626 cm^{-1} and on complexation was shifted to 631 and 630 cm^{-1} for Co(II) and Ni(II) complexes which indicated the coordination via pyridyl nitrogen atom [34]. The existence of coordinated water was proved by the appearance of the non-ligand band in the 987 and 926 cm^{-1} regions for Co(II) and Ni(II) complexes [35]. Appearance new bands in the spectra of Co(II) and Ni(II) complexes at 468 and 457 cm^{-1} were due to the formation of v(M-S) bonds [36]. The proof of coordination to the N

atom was provided by the occurrence of the bands 530 and 532 cm^{-1} in the IR spectra of the Co(II) and Ni(II) complexes due to ν(M-N) [37].

3.4 ^{1}H NMR study

^{1}H NMR spectrum of the synthesized ligand (L) was measured in $CDCl_3$, with TMS as internal standard. The spectrum of the prepared Schiff base ligand L displayed singlet signal at 4.32 ppm which was attributed to methyl protons of ligand L. The signal at 8.12 ppm was assigned to the azomethine proton (-CH=N-) [38]. Also, the spectrum showed a multiplet in the range 6.23-8.72 ppm corresponding to the aromatic protons and thiophene protons [39], and the appearance of a singlet signal at 9.53 ppm due to the proton of the NH_2 group of the ligand [40].

3.5 Mass spectra

The mass spectral analysis of the synthesized Schiff base ligand is essential as it is one of the methods to exactly confirm the proposed formula. The mass spectrum of the ligand, L (Fig. 2) showed an intense molecular ion peak at m/z 217.00 (35%) (calc. 217.28 amu) that indicates the formation of the desired compound with molecular formula $C_{11}H_{11}N_3S$ as suggested in Table 1.

3.6 Diffuse reflectance spectra

The diffuse reflectance of the Schiff base ligand (L) exhibited band at 245 nm attributed to π–π* transitions in both aromatic benzene and thiophene rings and azomethine (-C=N) group [41]. Another band was displayed at 345 nm referred to n–π* transitions of the lone pair of the nitrogen in the azomethine group and sulfur in the thiophene ring [42]. In the complexes these bands were shifted to lower wavelengths as an outcome of coordination when binding with metal, thus confirming the formation of Schiff base metal complexes (Table 3) [43]. The diffuse reflectance spectrum of the Co(II) complex, exhibits two peaks at 614 and 698 nm assigned to the transition $^4T_{1g}(F)\rightarrow{}^4T_{2g}(F)$ and$^4T_{1g}(F)\rightarrow{}^4A_{2g}(F)$, respectively suggesting an octahedral geometry for this complex [44]. The diffuse reflectance spectrum of Ni(II) complex showed two peaks around 505 and 636 nm, attributed to $^3A_{2g}(F) \rightarrow {}^3T_{2g}(F)$ and $^3A_{2g}(F)\rightarrow {}^3T_{1g}(P)$ transitions, respectively, indicating an octahedral geometry [45]. On the other hand, the diffuse reflectance spectra in both Co(II) and Ni(II) complexes showed two bands at 445 and 444 nm, respectively corresponding to charge transfer [46, 47].

Table 3
Electronic spectra data λ (nm) of the Schiff base (L) and its metal complexes.

Compound	λ_{max} (nm)			
	π-π*	n-π*	Charge transfer	d-d transition
L	245	345	---	---
$[CoL(H_2O)Cl_2].H_2O$	237	328	445	614, 698
$[NiL(H_2O)Cl_2].2H_2O$	229	330	444	505, 636

3.7 Fluorescence spectral studies

The fluorescence properties of the ligand L and its metal complexes were investigated in DMF at room temperature (Table 4). Generally, Schiff base systems exhibited fluorescence due to intra-ligand π–π* transitions, which showed an intense emission band at 347 nm upon photoexcitation at 309 nm. On the other hand, the excitation spectra of Co(II) and

Ni(II) complexes exhibited fluorescence emission bands at 370 and 455 nm when excited at 329 and 340 nm, respectively. It was found that the fluorescence emission intensity of Schiff-base decreased on complex formation with metal ions as clear from Fig. 3 [48, 49]. In general, all the synthesized compounds can serve as potential photoactive materials, as indicated by their characteristic fluorescence properties.

Table 4
Fluorescence data of the Schiff base and its metal complexes.

Compound	$\lambda_{excitation}$	$\lambda_{emission}$
L	309	347
$[CoL(H_2O)Cl_2].H_2O$	329	370
$[NiL(H_2O)Cl_2].2H_2O$	340	455

3.8 Thermal analyses

The thermal behaviors of the metal complexes were studied by using TG and DTG analyses, and the results were listed in Table 5 and represented in Fig. 4. The thermogram analysis (TGA/DTA) of the complexes is useful to prove the presence of water molecule inside or outside the coordination sphere and decomposition temperature of the compounds.

Table 5
Thermogravimetric data of the complexes.

Compound	Stage	Temp. range (°C)	Mass loss (%)		Evolved moiety	Residue (%) Found (Calcd.)
			Calcd	Found		
$[CoL(H_2O)Cl_2].H_2O$	I	48-125	4.72	5.114	H_2O (hyd.)	$CoC_{11}H_{11}N_3SCl_2$
	II	125-538	48.55	48.72	H_2O (coord.) Cl_2 and $C_5H_9N_2$	CoC_6H_2NS
	III	538-724	31.35	30.97	C_6H_2NS	Co 15.38% (15.19%)
$[NiL(H_2O)Cl_2].2H_2O$	I	47-213	13.47	13.82	$2H_2O$ (hyd.) and H_2O (coord.)	$NiC_{11}H_{11}N_3S\ Cl_2$
	II	213-429	15.33	14.94	½ Cl_2, and C_2H_2	$NiC_9H_9N_3S$ ½Cl_2
	III	429-726	56.24	55.86	½ Cl_2 and $C_9H_9N_3S$	Ni 15.38% (14.96%)

The thermogravimetric analysis of **$[Co(C_{11}H_{11}N_3S)(H_2O)Cl_2].H_2O$** complex involved three decomposition steps. The first step from 48-125 ºC range with a mass loss 5.11% (Calcd. 4.72%) due to the removal of a molecule of hydrating water. The second step appeared in the range 125-538 ºC with weight loss 48.72% (Calcd. 48.55%) corresponding to the loss of

a molecule of coordinated water, Cl_2 gas and $C_5H_9N_2$ species. The final step was demonstrated at 538-750 ºC which showed a loss mass of 30.97% (calcd. 31.35%) with the removal of C_6H_2NS species leaving cobalt metal as a final residue.

The thermal decomposition of the complex with the molecular formula **$[Ni(C_{11}H_{11}N_3S)(H_2O)\ Cl_2].2H_2O$** proceeds with three degradation steps. The first decomposition stage within the temperature range of 47-213 ºC which related to the evolution of 2 molecules of hydrated water and liberation of one molecule of coordinated water. Whereas, the second step in the temperature range 213-429 ºC which attributed to the liberation of ½ Cl_2 and C_2H_2 with mass loss of 14.94% (calcd. 15.33%). The final decomposition stage in the temperature range of 429-726 ºC attributed to the complete decomposition of a part of ligand leaving Ni as a final product.

3.9 Kinetic data

The kinetic thermodynamic parameters of decomposition processes of complexes such as the energy of activation (E*), enthalpy (ΔH*), entropy (ΔS*) and free energy change (Gibbs free energy) of decomposition (ΔG*) were evaluated graphically by employing the Coats–Redfern [50, 51] equation. The data were summarized in Table 6 of the supporting information.

Table 6
Thermodynamic data of the thermal decomposition of the complexes.

Compound	Stage	Decom.range. °C	A (S^{-1})	ΔH* (kJ/mol)	ΔS* (kJ/mol)	ΔG* (kJ/mol)	Ea (kJ/mol)	R^2
$[CoL(H_2O)Cl_2].H_2O$	I	64-326	$2.02x10^9$	686.53	-55.10	167	69.26	0.964
	II	326-537	$2.28x10^1$	337.58	-223.00	122	37.71	0.965
	III	537-724	$3.65x10^8$	156.64	-86.80	151	161.61	0.974
$[NiL(H_2O)Cl_2].2H_2O$	I	53-140	$3.37x10^7$	58.30	-90.00	212.09	59.05	0.969
	II	140-217	$1.15x10^{11}$	101.25	-28.91	106.41	102.74	0.976
	III	217-719	$5.99x10^2$	59.53	-197.14	171.64	64.26	0.981

Coats–Redfern equation

The Coats–Redfern equation, which is a typical integral method, can be represented as:

$$\int_0^{\alpha} \frac{d\alpha}{(1-\alpha)^n} = \frac{A}{\alpha}\int_{T_1}^{T_2} \exp\left(\frac{-E^*}{RT}\right) dt$$

For the convenience of integration, the lower limit T_1 is usually taken as zero. This equation on integration gives

$$\ln\left[\frac{-\ln(1-\alpha)}{T^2}\right] = \frac{-E^*}{RT} + \ln\left(\frac{AR}{\varphi E^*}\right)$$

If a plot of the left-hand side against 1/T was drawn, E* (the energy of activation in kJ mol^{-1}) was calculated from the slope and A in (s^{-1}) from the intercept (Fig. 5). The entropy of activation ΔS* (in J K^{-1} mol^{-1}) was calculated using the equation:

$$\Delta S^* + R \ln\left(\frac{Ah}{K_B T_s}\right)$$

where K_B is the Boltzmann constant, h is the Planck constant and T_s is the DTG peak temperature.

The entropy of activation was found to have negative values for Co(II) and Ni(II) complexes which indicated that decomposition reactions proceed with a lower rate than normal ones. Also, according to the kinetic data obtained, Co(II) and Ni(II) complexes have negative entropy, which indicated that activated complexes have more ordered systems than reactants.

The correlation coefficients of the Arrhenius plots of the thermal decomposition steps were found to range from 0.92-0.98, indicating good fitness of the linear function. From all the previous data, the proposed structures of the ligand and its complexes were given in Fig. 6.

3.10 Optical properties

The optical band energy gap (E_g) for the Co(II) and Ni(II) complexes can be determined based on the dependence of absorption coef□cient (α) on photon energy (hv). For transition, α is given by [52].

$(\alpha hv)^{2/n} = B\,(hv - E_g)$

Where α was the absorption coefficient and was calculated from the relation α = A/d (where A is the absorbance and d is the thickness of the cell), B is the optical constant, h is Planck's constant and □ was incident light frequency [53]. The optical absorption spectra of complexes were given in Fig. 7 and the values of bandgap energy for Co(II) and Ni(II) complexes were observed from the curves as 2.18 and 1.64, respectively. These results indicated that these complexes have highly efficient photovoltaic properties and could be used as semiconductors in solar cell programs [54, 55].

3.11 Metal uptake

The adsorption of Co(II) and Ni(II) ions with different concentrations (0.01M, 0.001M and 0.0001M) using ligand L was studied at different times 1, 2 and 5 hrs.

From the data, the results showed that the removal percentage of Co(II) and Ni(II) metal ions increased as time increased (Fig. 8). The highest removal percentage at 0.01 M of Co(II) and Ni(II) was found to be 45.6, 29.7% and at 0.001 M of the metal ion was 55.4, 53.2% and at 0.0001 M the removal was found 65.8, 68.6%, respectively. Also, the results appeared that the percentage of the removal of the metal ion increased as the concentration of metal ion decreased [56] (Fig. 9).

3.12 DFT study

3.12.1 Molecular DFT Calculation of Ligand

Figure 10 showed the optimized structures of the ligand as the lowest energy configurations. The natural charges obtained from Natural Bond Orbital Analysis (NBO) showed that the more negative active sites were in order N1 (-0.552), N2 (-0.426), N3 (-0.786) and S (0.452).

3.12.2 Molecular DFT Calculation of [CoL(H_2O)Cl_2] and [NiL(H_2O)Cl_2]

Figure 11 showed the optimized structures of the complexes as the lowest energy configurations. The cobalt and nickel atoms were six-coordinated in an octahedral geometry. The atoms N1, N2, S and O were almost in one plane deviated by -2.060° and -0.312°, respectively, Tables 7 and 8. The distances between N1----N2, N1----S and N2----S in the ligand (2.338, 5.151 and 4.000Å) are longer than those in the complexes [CoL(H_2O)Cl_2] (2.164, 3.914 and 2.719Å) and [NiL(H_2O)Cl_2] (2.132, 3.914 and 2.804Å) due to complex formation through N1, N2, S and O.

Table 7
Important optimized bond lengths (Å) and bond angles (°) of [CoL(H_2O)Cl_2].

Type of bond	**Bond length(Å) Complex**	**Type of bond**	**Bond length(Å) L Complex**
Co-N1	1.896	Co-*Cl*2	- 2.312
Co-N2	1.840		
Co-S	2.091	N1-----S	5.151 3.914
Co-O	2.028	N2-----S	4.000 2.719
Co-*Cl*1	2.335	N1-----N2	2.338 2.164
Type of Angle	Angle (°) Complex	Type of Angle	Angle (°) Complex
N1-Co-N2	70.79	*Cl*2-Co-N1	89.22
N1-Co-O	100.5	*Cl*2-Co-N2	94.91
N2-Co-S	87.26	*Cl*2-Co-O	82.65
O-Co-S	101.4	*Cl*2-Co-S	93.68
*Cl*1-Co-N1	87.10	N1-Co-S	158.0
*Cl*1-Co-N2	102.2	N2-Co-O	171.1
*Cl*1-Co-O	78.94	*Cl*1-Co-*Cl*2	160.2
*Cl*1-Co-S	96.98	N1-N2-S-O	-2.060*
*dihedral angle			

Table 8
Important optimized bond lengths (Å) and bond angles (°) of [NiL(H_2O)Cl_2].

Type of bond	Bond length(Å) Complex	Type of bond	Bond length(Å) L Complex	
Ni-N1	1. 821	Ni-*Cl*2	-	2.172
Ni-N2	1. 837			
Ni-S	2.151	N1-----S	5.151	3.914
Ni-O	1.795	N2-----S	4.000	2.804
Ni-*Cl*1	2.157	N1-----N2	2.338	2.132
Type of Angle	Angle (°) Complex	Type of Angle	Angle (°) Complex	
N1-Ni-N2	71.28	*Cl*2-Ni-N1	89.63	
N1-Ni-O	104.3	*Cl*2-Ni-N2	88.33	
N2-Ni-S	88.96	*Cl*2-Ni-O	91.08	
O-Ni-S	95.45	*Cl*2-Ni-S	89.72	
*Cl*1-Ni-N1	91.29	N1-Ni-S	160.2	
*Cl*1-Ni-N2	91.91	N2-Ni-O	175.6	
*Cl*1-Ni-O	88.75	*Cl*1-Ni-*Cl*2	179.1	
*Cl*1-Ni-S	89.40	N1-N2-S-O	-0.312*	
*dihedral angle				

The bonds attached to atoms coordinated to metal ions were elongated in complex (N1-C2, N1-C3, N2-C2, N2-C11, S-C6 and S-C9 are 1.417, 1.370, 1.413, 1.359, 1.843 and 1.751 Å in cobalt complex and 1.341, 1.365, 1.427, 1.282, 1.800 and 1.774 Å in nickel complex) compared to those in the free ligand (N1-C2, N1-C3, N2-C2, N2-C11, S-C6 and S-C9 are 1.337, 1.338, 1.400, 1.275, 1.758 and 1.735 Å) The angle C2-N2-C11 was decreased from 117.2 in the ligand to 101.4 and 100.7 in cobalt and nickel complexes, respectively, upon complex formation.

The natural charges computed from the NBO-analysis on the coordinated atoms were Co (+0.114), O(-0.677), N1(-0.695), N2(-0.765), S(0.671), *Cl*1(-0.478) and *Cl*2(-0.442) in case of [CoL(H_2O)Cl_2] and Ni (+0.037), O(-0.763), N1(-0.526), N2(-0.395), S(0.468), *Cl*1(-0.365) and *Cl*2(-0.404) in case of [NiL(H_2O)Cl_2], Fig. 11.

3.12.3 Molecular electrostatic potential and molecular orbital

Figure 11 showed the MEP surface is to locate the positive (blue color) and negative (red color, it is bound loosely or excess electrons) charged electrostatic potential in the molecule. The computed total energy, the highest occupied molecular orbital (HOMO) energies, the lowest unoccupied molecular orbital (LUMO) energies and the dipole moment for the ligands and complexes were calculated, Table 9. The more negative values of the total energy of the complexes than

that of the free ligand indicate that the complexes are more stable than the free ligands and the energy gaps ($E_g = E_{LUMO} - E_{HOMO}$) are smaller in case of complexes than that of ligand due to chelation of ligand to metal ions, Table 9. The lowering of E_g in complexes compared to that of ligand explains the charge transfer interactions upon complex formation, Fig. 12.

Table 9
Calculated energies and properties of ligand, $[CoL(H_2O)Cl_2]$ and $[NiL(H_2O)Cl_2]$.

Property	L	$[CoL(H_2O)Cl_2]$	$[NiL(H_2O)Cl_2]$
The total energy E (a.u.)	-988.409	-2130.196	-2154.325
HOMO (eV)	-5.7495	-5.0211	-4.4284
LUMO (eV)	-1.8422	-3.1157	-2.4180
$E_g=E_{LUMO}- E_{HOMO}$ (eV)	3.9073	1.9054	2.0104
Dipole moment (Debye)	4.5942	3.4793	2.4419
ionization potential $I=-E_{HOMO}$	5.7495	5.0211	4.4284
electron affinity $A=-E_{LUMO}$	1.8422	3.1157	2.4180
Electronegativity $\chi=(I+A)/2$	3.7958	4.0684	3.4232
chemical hardness $\eta=(I-A)/2$	1.9536	0.9527	1.0052
chemical softness $S=1/2\eta$	0.2559	0.5248	0.4974
chemical potential $\mu=-\chi$	-3.7958	-4.0684	-3.4232
Electrophilicity $\omega = \mu2/2\eta$	3.6876	8.6868	5.8288

3.12.4 Reactivity studies

Many reactivity descriptors such as ionization potential (I), electron affinity (A), Electronegativity (χ), chemical potential (μ), hardness (η), softness (S) and electrophilicity index (ω), all derived from the HOMO and LUMO energies, have been proposed for understanding various aspects of reactivity associated with chemical reactions, Table 9.

3.13 Antimicrobial activities

The antibacterial activity of the Schiff base ligand and its complexes

were tested against two gram-positive bacteria (*S. aureus* and *B. subtilis*), two gram-negative bacteria *(P. vulgaris* and *E. coli*) and two fungi (*A. flavus* and *C. albicans*) (Fig. 13). The inhibition zone diameter (mm) of all investigated compounds in addition to the calculated percent activity index data were listed in Table 10. The activity index was calculated by the following relation [57]: A=I/I□*100, where A= Activity index, I= Inhibition zone of the compound (mm) and I□= Inhibition zone of the standard drug (mm) (Fig. 14).

Table 10
Antimicrobial assay of the free ligand, L and its metal complexes

Compound	**Zones diameter showing complete growth inhibition in mm***					
	Gram-positive bacteria		**Gram-negative bacteria**		**Fungi**	
	Staphylococcus aureus **RCMB 010010**	***Bacillus subtilis*** **RCMB 015**	***Proteus vulgaris*** **RCMB 004**	***Escherichia coli*** **RCMB 010052**	***Aspergillus flavus*** **RCMB 002002**	***Candida albicans*** **RCMB 005003**
L	11(46)	15 (58)	13(52)	NA	NA	NA
$[CoL(H_2O)Cl_2].H_2O$	17 (71)	18 (69)	16 (64)	20 (67)	8 (50)	12 (60)
$[NiL(H_2O)Cl_2].2H_2O$	11 (46)	15 (58)	14 (56)	16 (53)	13 (81)	13 (65)
Gentamycin(a)	24	26	25	30	–	–
Ketoconazole(b)	–	–	–	–	16	20
DMF(c)	–	–	–	–	–	–
The test was done using the agar well diffusion method. *% Activity index are in parentheses.						
(a)Reference standards for bacteria.						
(b)Reference standards for fungi.						
(c) Dimethyl formamide was used as a negative control.						
Inhibition zone value: NA: No activity; ≤ 1/4 control zone diameter: low activity;						
≤ 1/2 control zone diameter: intermediate activity; ≤ 3/4 control zone diameter: high activity.						
>3/4 control zone diameter: very high activity.						

3.13.1 Effect of bacteria

The results revealed that:

- The Schiff base ligand showed remarkable potential activity against all bacteria under study except *E. coli*. It was a moderate activity against *B. subtilis* which has an activity index of about (58%).

- Co(II) and Ni(II) tested complexes, showed greater bacterial activities than the Schiff base ligand against all tested bacteria.
- Co(II) complex has the highest activity against all the studied bacteria than Ni(II) complex.

3.13.2 Effect of fungi

- The Schiff base ligand showed a zero activity index against the tested fungi.
- The activity index of Co(II) and Ni(II) complexes against *C. albicans* are 60 and 65, respectively, which is moderate to the reference drug (Ketoconazole).
- Ni(II) complex showed the highest activity against all tested fungi than Co(II) complex.

3.14 Molecular docking studies

Molecular docking studies were achieved with MOA2019 software [24], to find out the possible binding modes of the ligand and the complexes with the receptor of gram –ve bacteria (Escherichia coli) (PDB ID: 1fj4) [25] and gram +ve bacteria (Bacillus subtilis) (PDB ID: 1QD9) [26], Tables 11 and 12.

Table 11
The Docking interaction data calculations of L, $[CoL(H_2O)Cl_2]$ and $[NiL(H_2O)Cl_2]$ with the active sites of Escherichia coli (gram –ve bacteria) TRANSFERASE (PDB ID: 1fj4).

	Receptor	Interaction	Distance(Å)*	E (kcal/mol)
L				
N 13	O GLY 205	H-donor	3.18 (2.31)	-1.1
5-ring	CG2 THR 302	pi-H	3.73	-0.8
5-ring	CE1 PHE 392	pi-H	3.77	-0.5
$[CoL(H_2O)Cl_2]$				
O 30	OD1 ASP 70	H-donor	2.59 (1.61)	-18.9
N 15	OD2 ASP 70	H-donor	3.32 (2.36)	-3.32
CL 28	O LEU 54	H-donor	3.09 (3.09)	-3.09
N 15	OD2 ASP 70	Ionic	3.32	-2.7
O 30	OD1 ASP 70	Ionic	2.59	-7.9
O 30	OD2 ASP 70	Ionic	3.00	-4.5
$[NiL(H_2O)Cl_2]$				
N 15	OD1 ASP 293	H-donor	2.94 (1.98)	-5.7
O 30	OD1 ASP 293	H-donor	2.64 (1.74)	-17.2
N 15	OD1 ASP 293	Ionic	2.94	-4.9
O 30	OD1 ASP 293	Ionic	2.64	-7.4
*The lengths of H-bonds are in brackets.				

Table 12
The Docking interaction data calculations of L, [CoL(H_2O)Cl_2] and [NiL(H_2O)Cl_2] with the active sites of the receptor of Bacillus subtilis (gram +ve bacteria) gene regulation (PDB ID: 1QD9).

	Receptor	Interaction	Distance(Å)*	E (kcal/mol)
L				
O 23	OD1 ASN 25 (A)	H-donor	2.77 (1.81)	-1.9
N 17	ND2 ASN 24 (C)	H-acceptor	3.08 (2.15)	-2.1
[CoL(H_2O)Cl_2]				
N 15	OD2 ASP 80 (A)	H-donor	2.87 (1.75)	-3.7
O 30	OD2 ASP 80 (A)	H-donor	2.60 (2.11)	-15.2
N 4	OD2 ASP 80 (A)	Ionic	3.02	-4.3
S 13	OD1 ASP 80 (A)	Ionic	3.11	-3.8
S 13	OD2 ASP 80(A)	Ionic	3.35	-2.5
N 15	OD2 ASP 80 (A)	Ionic	2.87	-5.4
O 30	OD2 ASP 80 (A)	Ionic	2.60	-7.8
[NiL(H_2O)Cl_2]				
O 30	OE2 GLU 119 (C)	H-donor	2.71 (1.81)	-16.6
N 4	OE2 GLU 119 (A)	Ionic	3.38	-2.4
S 13	OE2 GLU 119 (B)	Ionic	2.88	-5.4
N 14	OE2 GLU 119 (B)	Ionic	3.73	-1.1
O 30	OE2 GLU 119 (C)	Ionic	2.71	-6.8
*The lengths of H-bonds are in brackets.				

The binding free energy of the ligand and its metal complexes with protein (PDB ID: 1fj4) receptor of gram –ve bacteria (Escherichia coli) were found to be -2.4, -40.41 and -35.2 kcal/mol for L, [CoL(H_2O)Cl_2] and [NiL(H_2O)Cl_2]; respectively, Table 11. Also, the binding free energies of the ligand and its metal complexes with protein (PDB ID: 1QD9) receptor of gram +ve bacteria (Bacillus subtilis) are found to be -4.0, -44.6 and -32.3 kcal/mol for L, [CoL(H_2O)Cl_2] and [NiL(H_2O)Cl_2], respectively, Table 12. The more negative the binding energy the stronger interaction. So, the interactions were in the order of [CoL(H_2O)Cl_2] □ [NiL(H_2O)Cl_2] □ L for both cases.

The 2D and 3D plots of the interaction of L, [CoL(H_2O)Cl_2] and [NiL(H_2O)Cl_2] with the active site of the receptor of Escherichia coli and Bacillus were shown in Figs. 15 and 16, respectively.

References

1. M. Abu-Dief, I.M.A. Mohamed, A review on versatile applications of transition metal complexes incorporating Schiff bases. Beni-Suef Univ. J. of. Basic and Appl. Sci. **4**, 119-133 (2015). https://doi.org/10.1016/j.bjbas.2015.05.004.

2. M. Yadav, Synthesis, Characterization, and Biological Activity of Some Transition Metal Complexes of N-Benzoyl-N-2-thiophenethiocarbohydrazide. Inter. J. of Inorg. Chem. **2012**, 1-8 (2012). https://doi.org/10.1155/2012/269497.
3. M.M. Singh, R.B. Rastogi, B.N. Upadhyay, M. Yadav, Thiosemicarbazide, phenyl isothiocyanate and their condensation product as corrosion inhibitors of copper in aqueous chloride solutions. Materials Chem. and Phy. **80** (1), 283–293(2003). https://doi.org/ 10.1016/S0254-0584(02)00513-8.
4. R.B. Rastogi, M.M. Singh, M. Yadav, K. Singh, Substituted Dithiobiurets, their Molybdenum and Tungsten Complexes as Corrosion Inhibitors for Mild Steel in Sulphuric Acid. Portugaliae Electrochimica Acta **22**(2), 127-147(2004). https://doi.org/ 10.4152/pea.200402127.
5. R.B. Rastogi, M. Yadav, A. Bhattacharya, Application of molybdenum complexes of 1-aryl-2,5-dithiohydrazodicarbonamides as extreme pressure lubricant additives. Wear. **252** (9-10), 686–692 (2002). https://doi.org/10.1016/s0043-1648(01)00878-x.
6. N. Siddiqui, W. Ahsan, Triazole incorporated thiazoles as a new class of anticonvulsants: Design, synthesis and in vivo screening. European J. of Medic. Chem. **45**, 1536–1543 (2010). https://doi.org/ 10.1016/j.ejmech.2009.12.062.
7. H.M. Parekh, M.N. Patel, Preparation of Schiff's base complexes of Mn(II), Co(II), Ni(II), Cu(II), Zn(II), and Cd(II) and their spectroscopic, magnetic, thermal, and antifungal studies. Russian J. of Coord. Chem. **32**, 431–436 (2006). https://doi.org/ 10.1134/S1070328406060066.
8. P.K. Panchal, P.B. Pansuria, M. N. Patel, In-vitro biological evaluation of some ONS and NS donor Schiff 's bases and their metal complexes. J. of Enz. Inhib. and Medic. Chem. **21**(4), 453–458 (2006). https://doi.org/ 10.1080/14756360600628551.
9. J. Chakrborty, M. Nandi, H. Mayer Figgie, W.S. Sheldric, L. Sorane, A. Bhaymik, P. Banerjee, Nickel Complexes with N_2O Donor Ligands: Syntheses, Structures, Catalysis and Magnetic Studies. Eur. J. Inorg. Chem. **32**, 5033(2007). https://doi.org/10.1002/ejic.200700500.
10. N.V. Kulkarni, M.P. Satisha, S. Budagumpi, G.S. Kurdekar V.K. Revankar, Binuclear transition metal complexes of bicompartmental SNO donor ligands: Synthesis, characterization, and electrochemistry. J. Coord. Chem. **63**, 1451(2010). https://doi.org/10.1080/00958971003770405.
11. R.R. Coombs, S.A. Westcott, A. Decken, F. Baerlocher, Palladium(II) Schiff base complexes derived from sulfanilamides and aminobenzothiazoles. J. Trans.Met. Chem. **30**, 411(2005). https://doi.org/ 10.1007/s11243-004-7625-4.
12. M.M. Omar, G.G. Mohammed, Potentiometric, spectroscopic and thermal studies on the metal chelates of 1-(2-thiazolylazo)-2-naphthalenol. Spectrochim. Acta **61**A, 929 (2005). https://doi.org/10.1016/j.saa.2004.05.040.
13. R.C. Maurya, D.D. Mishra, S. Mukherjee and J. Dubey, Metal cyanonitrosyl complexes: synthesis, magnetic and spectral studies of some novel mixed-ligand cyanonitrosyl $[CoNO]_8$ complexes of cobalt(I) with heterocyclic bases. polyhedron **14**(10), (1995). https://doi.org/10.1016/0277-5387(94)00394-T.
14. J. Bassett, R.C. Denney, G.H. Jeffery, J. Mendham, Vogel's Textbook of Quantitative Inorganic Analysis Including Instrumental Analysis: (ELBS and Longman Group Ltd. London) (1978) (a) 473, (b) 447, (c) 483.
15. P. Mittal, S. Joshi, V. Panwar, V.Uma, Biologically active Co (II), Ni (II), Cu (II) and Mn(II) Complexes of Schiff Bases derived from Vinyl aniline and Heterocyclic Aldehydes. Inter. J. of Chem.Tech. Res. **1**(2), 225-232 (2009). https://doi.org/10.1.1.595.843.
16. A.A. Mandour, N. Nabil, H.E. Zaazaa, M. Abdelkawy, Review on analytical studies of some pharmaceutical compounds containing heterocyclic rings: brinzolamide, timolol maleate, flumethasone pivalate, and clioquinol. Future J.of Pharma. Sci. **6**(52), 1-10 (2020). https://doi.org/10.1186/s43094-020-00068-4.
17. A.S Tapkir , S.S Chitlange , R.P Bhole, Discovery of Thiazole Based Bis Heterocyclic System for Anti- Inflammatory Potential. Antiinflamm. Antiallergy Agents Med. Chem. **16**(3), 175-192

(2017). https://doi.org/10.2174/1871523016666171114165958.

18. M. Hossain, A.K. Nanda, A Review on Heterocyclic: Synthesis and Their Application in Medicinal Chemistry of Imidazole Moiety. Sci. J. of Chem. **6**(5), 83-94 (2018). https://doi.org/10.11648/j.sjc.20180605.12.
19. M.N. Patel, P.S. Karia, P.A.Vekariya, A.P. Patidar, Synthesis of heterocyclic compounds and its applications. Arabian J. of Chem. **12**, 2983–2991 (2019). https://doi.org/10.1016/j.arabjc.2015.06.031.
20. A.I. Vogel, third ed., Longman ELBS, London, 5 th Ed.,John Wiley and Sons, Inc., New York, (1989).
21. E.T. Aljohani, M.R. Shehata, F. Alkhatib, S.O. Alzahrani, A. M. Abu Dief, Development and structure elucidation of new VO^{2+}, Mn^{2+} , Zn^{2+}, and Pd^{2+} complexes based on azomethine ferrocenyl ligand: DNA interaction, antimicrobial, antioxidant, anticancer activities, and molecular docking. Appl. Organomet. Chem. **35**, 1-24 (2021). https://doi.org/ 10.1002/aoc.6154.
22. M. J. Frisch, G. W. Trucks, H. B. Schlegel, G. E. Scuseria, M. A. Robb, J. R. Cheeseman, G. Scalmani, V. Barone, G. A. Petersson, H. Nakatsuji, X. Li, M. Caricato, A. Marenich, J. Bloino, B. G. Janesko, R. Gomperts, B. Mennucci, H. P. Hratchian, J. V. Ortiz, A. F. Izmaylov, et al., Gaussian 09, Revision A.02 (Gaussian, Inc., Wallingford CT), (2016). https://gaussian.com/g09citation/
23. A.A. Abou-Hussein, W. Linert, Synthesis, spectroscopic studies and inhibitory activity against bacteria and fungi of acyclic and macrocyclic transition metal complexes containing a triamine coumarine Schiff base ligand, Spectrochimica Acta A **141**, 223-232 (2015).
24. Molecular Operating Environment (MOE), 2019.01; Chemical Computing Group ULC, 1010 Sherbrooke St. West, Suite #910, Montreal, QC, Canada, H3A 2R7, (2021). https://www.chemcomp.com/Research-Citing_MOE.htm.
25. A.C. Price, K.H. Choi, R.J. Heath, Z. Li, S.W. White, C.O. Rock, Inhibition of β-ketoacyl-acyl carrier protein synthases by thiolactomycin and cerulenin: structure and mechanism. J. Biol. Chem. **276**, 6551 (2001). https://doi.org/ 10.1074/jbc.M007101200.
26. S. Sinha, P. Rappu, S.C. Lange, P. Mäntsälä, H. Zalkin, J.L. Smith, Crystal structure of Bacillus subtilis YabJ, a purine regulatory protein and member of the highly conserved YjgF family. **96**(23), 13074–13079 (1999). https://doi.org/10.1073/pnas.96.23.13074.
27. N.N. Jha, I.P. Ray, Magnetic studies of Co(II) and Ni(II) complexes of hydroxamic acid. Asian J. of Chem. **12**(3), 703-706 (2000). https://asianjournalofchemistry.co.in/User/ViewFreeArticle.aspx?ArticleID=12_3_16
28. N.P. Singh, Anu, J.V. Singh, Magnetic and spectroscopic studies of the synthesized metal complexes of bis(pyridine-2-carbo) hydrazide and their antimicrobial studies. E-J. of Chem., **9** (4), 1835–1842 (2012). https://doi.org/10.1155/2012/521345.
29. J. Singh, and P. Singh, Synthesis, Spectroscopic Characterization, and In Vitro Antimicrobial Studies of Pyridine-2-Carboxylic Acid N-(4-Chloro-Benzoyl)-Hydrazide and Its Co(II), Ni(II), and Cu(II) Complexes. Hindawi Publishing Corpor. Bio. Chem. and Appl. **7**, (2012). https://doi.org/10.1155/2012/104549.
30. O.A.M. Ali, S.M. El-Medani, D.A. Ahmed, D.A. Nassar, Synthesis, characterization, fluorescence and catalytic activity of some new complexes of unsymmetrical Schiff base of 2-pyridinecarboxaldehyde with 2,6-diaminopyridine. Spectrochimica Acta Part A **144**, 99–106 (2015). https://doi.org/10.1016/j.saa.2015.02.078.
31. O.A.M. Ali, S.M. El-Medani, D.A. Ahmed, D.A. Nassar, Metal carbonyl complexes with Schiff bases derived from 2-pyridinecarboxaldehyde: syntheses, spectral, catalytic activity and antimicrobial activity studies. J. of Mol. Str. **1074** (25), 713-722 (2014). https://doi.org/ 10.1016/j.molstruc.2014.05.035.
32. B. Kurt, H. Temel, M. Atlan, S. Kaya, Synthesis, characterization, DNA interaction and docking studies of novel Schiff base ligand derived from 2, 6-diaminopyridine and its complexes. J. of Mol. Str. **1209**, 127928 (2020).https://doi.org/1016/j.molstruc.2020.127928.

33. X. Li, Ch.-H. Li, J.-H. Jiang, H.-W. Gu, D.-L. Wei, L.-J. Ye, J.-L. Hu, S.-X. Xiao, D.-C. Guo, X. Li, H. Zhang, Q.-G Li, Synthesis and microcalorimetric determination of the bioactivities of a new Schiff base and its bismuth(III) complex derived from o-vanillin and 2,6-pyridinediamine. J. Therm. Anal. Calorim. **127**, 1767–1776 (2017). https://doi.org/10.1007/s10973-016-5892-x.

34. D.I. Tofiq, H.Q. Hassan, K.A. Abdalkarim, Preparation of a novel Mixed-Ligand divalent metal complexes from solvent free Synthesized Schiff base derived from 2,6-Diaminopyridine with cinnamaldehyde and 2,20-Bipyridine: Characterization and antibacterial activities. Arab. J. of Chem. **14**, 103429 (2021). https://doi.org/10.1016/j.arabjc.2021.103429.

35. G.G. Mohamed, H.A.E. Attia, N.A. Ibrahim, Synthesis, Characterization and Fungicidal Potentialities of some Transition Metal Complexes of Benzimidaz-oledithiocarbamate Based Ligand. Egypt. J. Agric. Res. **96** (2), 527-543 (2018). https://doi.org/ 10.21608/ejar.2018.135726.

36. M. Shakira, A. Abbasia, M. Azama, A.U. Khanb, Synthesis, spectroscopic studies and crystal structure of the Schiff base ligand L derived from condensation of 2-thiophenecarboxaldehyde and 3,3-diaminobenzidine and its complexes with Co(II), Ni(II), Cu(II), Cd(II) and Hg(II): Comparative DNA binding studies of L and its Co(II), Ni(II) and Cu(II) complexes. Spectrochimica Acta A **79**, 1866–1875 (2011). https://doi.org/10.1016/j.saa.2011.05.077.

37. A.P. Mishra, A. Tiwari, S.K. Gupta, R. Jain, Synthesis, Spectral and Antimicrobial Studies of some Co(II), Ni(II) and Cu(II) Complexes Containing 2-Thiophenecarboxaldehyde Moiety. E-J. of Chem. **9**(3), 1113-1121(2012). https://doi.org/10.1155/2012/585827.

38. N. Sari and P. G¨urkan, Some Novel Amino Acid-Schiff Bases and their Complexes Synthesis, Characterization, Solid State Conductivity Behaviors and Potentiometric Studies. Article in Z. Naturforsch. **59**b, 692 – 698 (2004). https://doi.org/ 10.1515/znb-2004-0610.

39. A.M. Daoud, H.A. Mahdi, Synthesis, characterization and evaluation biological activity of new Schiff base compounds and their complexes with some transition elements. J.Thi-Qar Sci. **6** (2), 81-89 (2017). https://www.jsci.utq.edu.iq/index.php/main/article/view/7.

40. L.W. Mohammed, A.A. Irzoqi, New 3- hydrazonoindolin-2-one Cd(II) complexes with amino pyridine ligands, Synthesis, Characterization and biological activity evaluation. Tikrit J. of Pure Sci. **25** (2), (2020). https://doi.org/10.25130/tjps.25.2020.028.

41. M. Usharani, E. Akila, R. Rajavel, Dinuclear Cu(II), Co(II), Ni(II) and Mn(II) complexes Framework Based on 1-(2-hydroxyphenyl) ethanone ligand: Synthesis, Structural Investigation and Biological properties. Int. J. Pharm. Sci. Rev. Res. **21**(2), 274-280 (2013). http://globalresearchonline.net/journalcontents/v21-2/49.pdf

42. M.A. Ayoub, E. H. Abd-Elnasser, M.A. Abedel-aziz, M.G. Rizk, Synthesis, Physicochemical, Thermal and Fluorescence Studies of Cobalt(II) Complex with Tridentate (ONS) Schiff Base Ligand Derived From 2-Aminophenol and 2-Acetylthiophene. J. of Scientific Res. in Sci. Article 35, **33**(1), 434-448 (2016). https://doi.org/ 10.21608/JSRS.2016.18341.

43. O.A.M. Ali, Z.H. Abd El Wahab, B.A. Ismail, Synthesis, structural characterization and evaluation of catalytic and antimicrobial properties of new mononuclear Ag(I), Mn(II), Cu(II) and Pt(IV) complexes. J. of Mol. Str. **1139**, 175-195 (2017). https://doi.org/ 10.1016/j.molstruc.2017.03.025.

44. Z.H. Abd El-Wahab, M.M. Marshaly, A.A. Salman, B.A. El-Shetary, A.A. Faheim, Co(II), Ce(III) and UO 2(VI) bis-salicylatothiosemicarbazide complexes: Binary and ternary complexes, thermal studies and antimicrobial activity. Spectrochimica Acta A **60**, 2861–2873 (2004). https://doi.org/ 10.1016/j.saa.2004.01.021.

45. A. S. Megahed, M. S. Al-Amoudi, M. S. Refat, A modern technique for preparation of zinc(II) and nickel(II) nanometric oxides using Schiff base compounds: synthesis, characterization, and antibacterial properties. Res. Chem. Intermed. 40, 1425–1439 (2014). https://doi.org/ 10.1007/s11164-013-1049-8.

46. N. Mondal, D.K. Dey, S. Mitra, K.M. Abdul Malik, Synthesis and structural characterization of mixed ligand [1]-2-hydroxy- acetophenone complexes of cobalt(III). Polyhedron **19**, 2707–2711 (2000). https://doi.org/10.1016/S0277-5387(00)00584-2.
47. M.A. Ayoub, E.H. Abd-Elnasser, M.A. Ahmed, M.G. Rizk, Some new metal(II) complexes based on bis-Schiff base ligand derived from 2-acetylethiophine and 2,6-diaminopyridine: Syntheses, structural investigation, thermal, fluorescence and catalytic activity studies. J. of Mol. Str. **1163**, 379-387 (2018). https://doi.org/10.1016/j.molstruc.2018.03.006.
48. P. Kavitha, M.R. Chary, B.V.V.A. Singavarapu, K.L. Reddy, Synthesis, characterization, biological activity and DNA cleavage studies of tridentate Schiff bases and their Co(II) complexes. J. of Saudi Chem. Soc. **20**, 69–80 (2016). https://doi.org/10.1016/j.jscs.2013.03.005.
49. A. Ashraf, M. Islam, M. Khalid, A.P. Davis, M.T. Ahsan, M. Yaqub, A. Syed, A.M. Elgorban, A.H. Bahkali, Z. Shafq, Naphthyridine derived colorimetric and fuorescent turn of sensors for Ni^{2+} in aqueous media. Scientific Rep. **11** (19242), 1-13 (2021) . https://doi.org/10.1038/s41598-021-98400-2.
50. F.A. Al-Saif, Spectroscopic elucidation, conductivity and activation Thermodynamic parameters studies on Pt (IV), Au (III) and Pd (II) 1, 5-dimethyl-2-phenyl-4-[(thiophen-2-ylmethylene)-amino]-1, 2-dihydro-pyrazol-3-one Schiff base complexes. Int. J. Electro. chem. Sci. **9**, 398-417 (2014). https://doi.org/10.1016/j.molliq.2018.06.077.
51. F.D. Firuzabadi, Z. Asadi, R. Yousefi, Synthesis of new nano Schiff base complexes: X-ray crystallography, thermal, electrochemical and anticancer studies of nano uranyl Schiff base complexes. Bulletin of the Chemical Society of Ethiopia **32**(1), 89-100 (2018). https://doi.org/10.4314/bcse.v32i1.8.
52. J.I. Pankove, Optical Processes in Semiconductors, Prentice-Hall Inc., New Jersey, (1971).
53. F. Karipcin, B. Dede, Y. Caglar, D. Hur, S. Ilican, M. Caglar, Y. Sahin, A new dioxime ligand and its trinuclear copper(II) complex: Synthesis, characterization and optical properties. Optics Commu. **272**, 131–137 (2007). https://doi.org/10.1016/j.optcom.2006.10.079.
54. M.M. Rashad, A.M. Hassan, A.M. Nassar, N.M. Ibrahim, A. Mourtada, A new nano-structured Ni(II) Schiff base complex: synthesis, characterization, optical band gaps, and biological activity. Apply Phys A **117**, 877–890 (2014). https://doi.org/10.1007/s00339-014-8448-6.
55. N.M. Hosny, E. Othman, F.I. El Dossoki, $[Cd(Anthranilate)_2]H_2O$ as a precursor of CdO nanoparticles. J. Mol. Struct. **1195**, 723–732 (2019). https://doi.org/ 10.1016/j.molstruc.2019.06.041.
56. F. Degryse, E. Smolders, D.R. Parker, Metal complexes increase uptake of Zn and Cu by plants: implications for uptake and deficiency studies in chelator-buffered solutions, Plant Soil **289**, 171–185 (2006). https://doi.org/10.1007/s11104-006-9121-4.
57. W.H. Mahmoud, G.G. Mohamed, H.A. Elsawy, M.A. Radwan, Metal complexes of novel Schiff base derived from the condensation of 2-quinoline carboxaldehyde and ambroxol drug with some transition metal ions. Appl. Organomet. Chem. **32**(7), 4392–4406 (2018). https://doi.org/10.1002/aoc.4392.

Figures

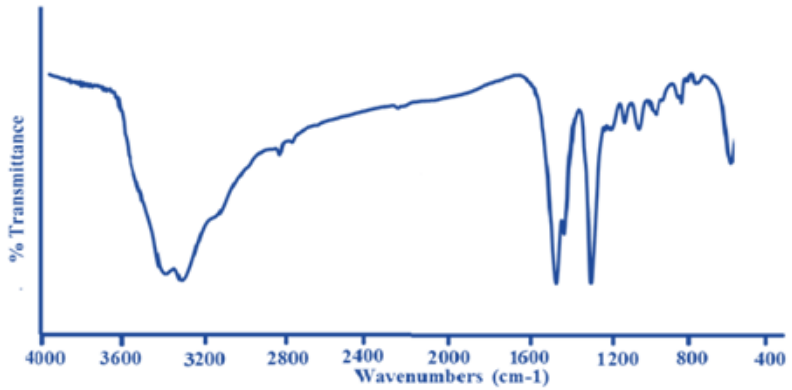

Figure 1

IR spectrum of the synthesized ligand (L).

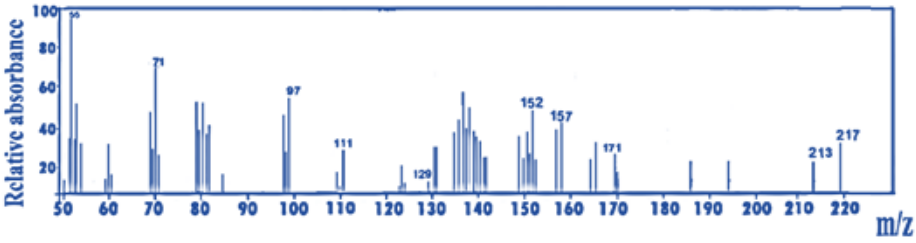

Figure 2

Mass spectrum of the synthesized ligand (L).

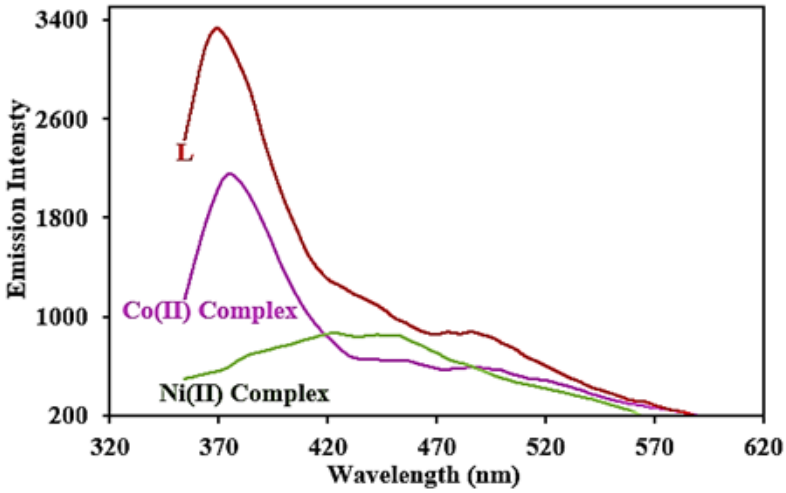

Figure 3

Fluorescence spectra of the synthesized ligand (L) and its Co(II) and Ni(II) complexes.

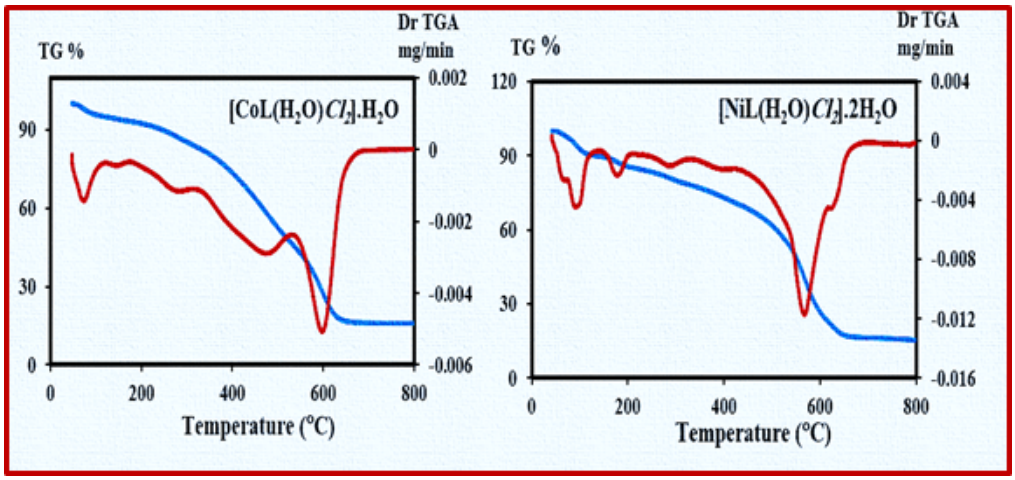

Figure 4

TG-DT thermograms of the Co(II) and Ni(II) complexes.

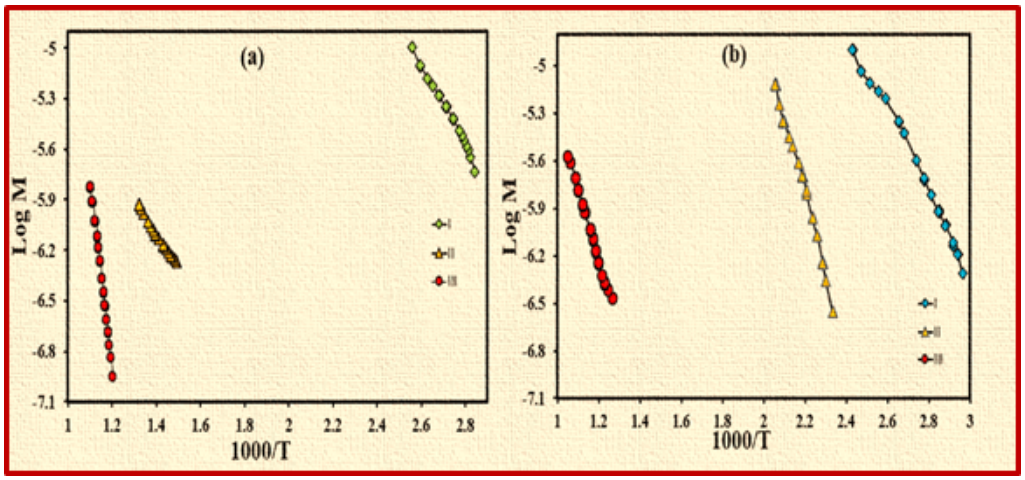

Figure 5

Coats-Redfern plots of (a) **$[CoL(H_2O)Cl_2].H_2O$,** (b) **$[NiL(H_2O)Cl_2].2H_2O$,** complexes (log M = $\log[\log\{W_\infty(W_\infty - W)^{-1}\}T^{-2}]$).

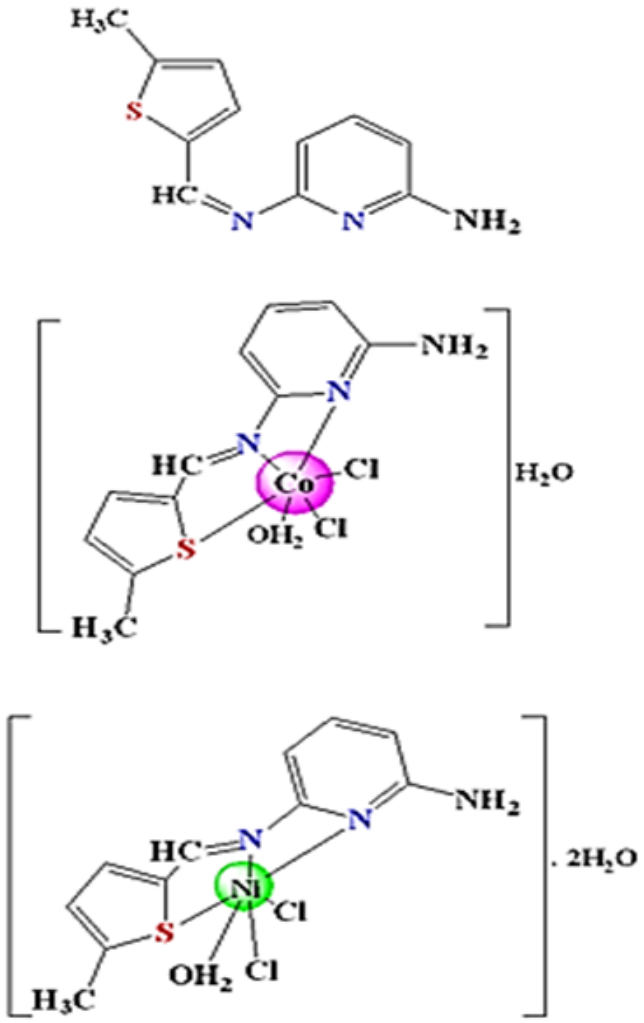

Figure 6

The propose structure of the Schiff base ligand (L) and its Co(II) and Ni(II) complexes.

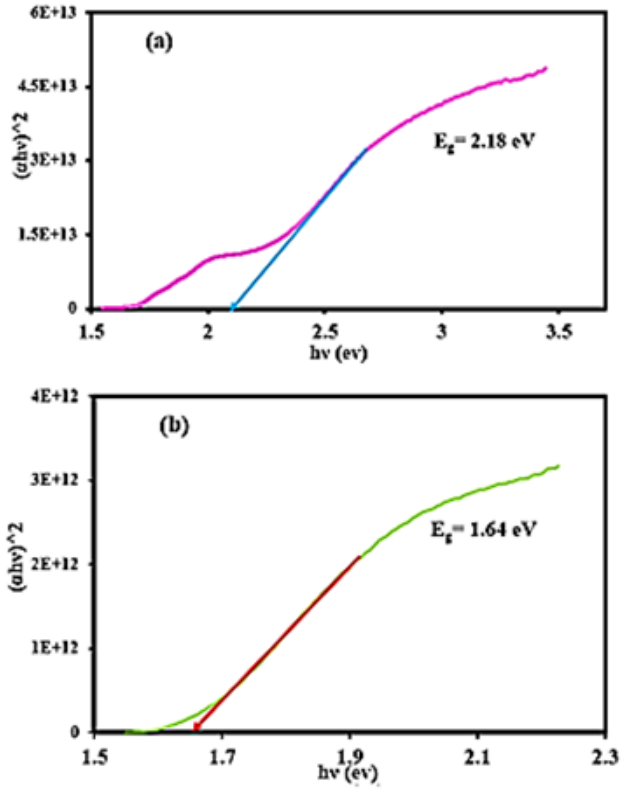

Figure 7

Optical band gap of (a) $[CoL(H_2O)Cl_2].H_2O$, (b) $[NiL(H_2O)Cl_2].2H_2O$.

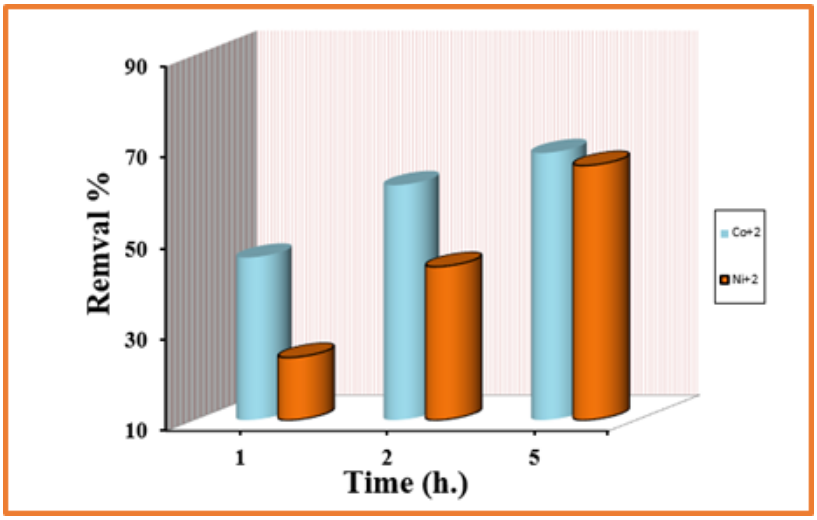

Figure 8

The efficiency of removal Co(II) and Ni(II) complexes at different times.

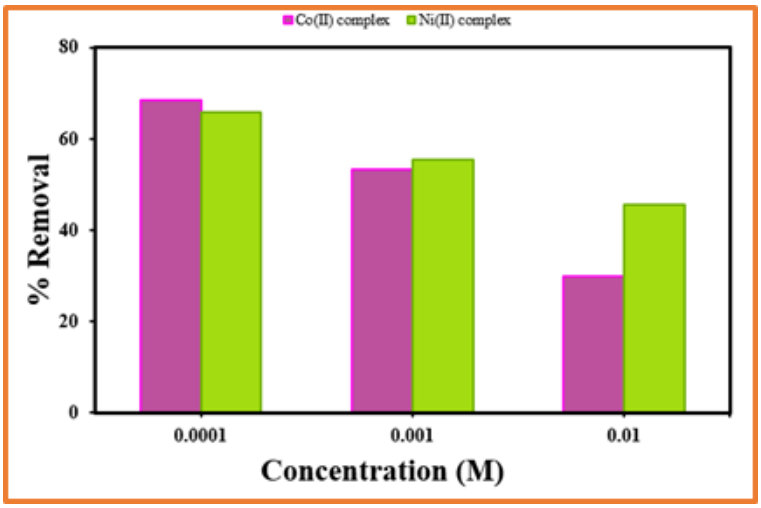

Figure 9

The efficiency of removal Co(II) and Ni(II) complexes at different concentrations of L.

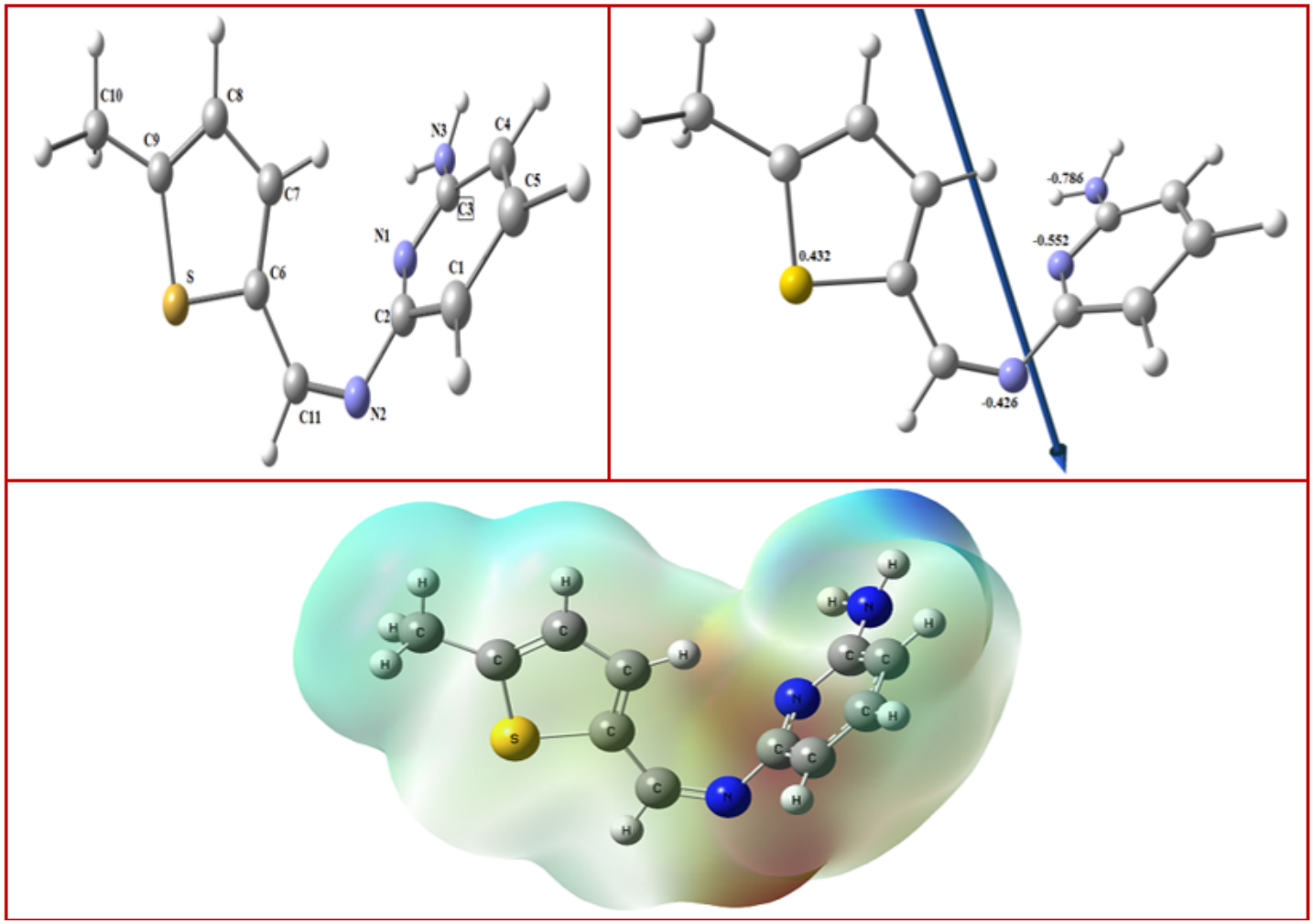

Figure 10

The optimized structure, the vector of the dipole moment, the natural charges on active centers and Molecular electrostatic potential (MEP) surface of ligand.

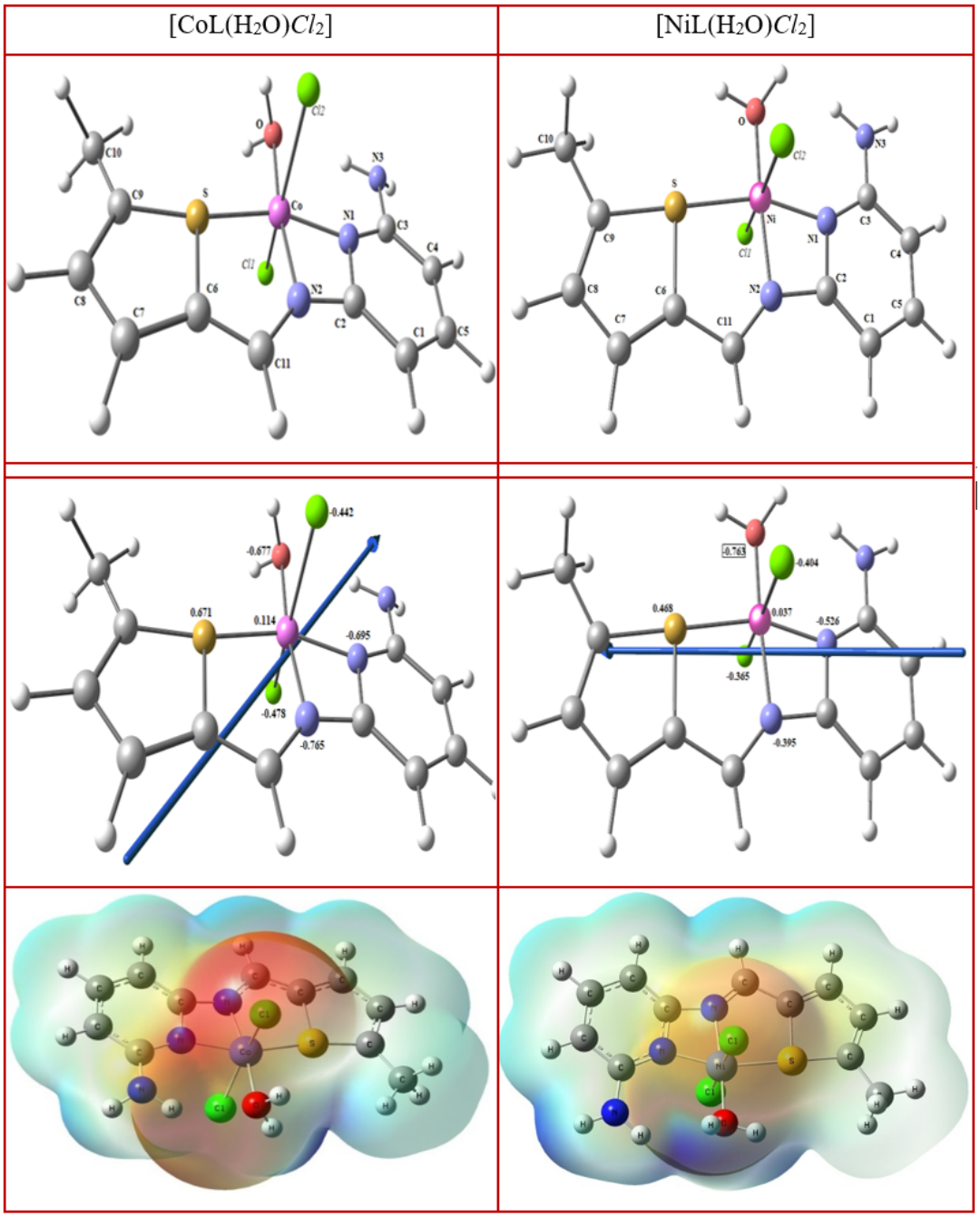

Figure 11

The optimized structure, the vector of the dipole moment, the natural charges on active centers and Molecular electrostatic potential (MEP) surface of $[CoL(H_2O)Cl_2]$ and $[NiL(H_2O)Cl_2]$.

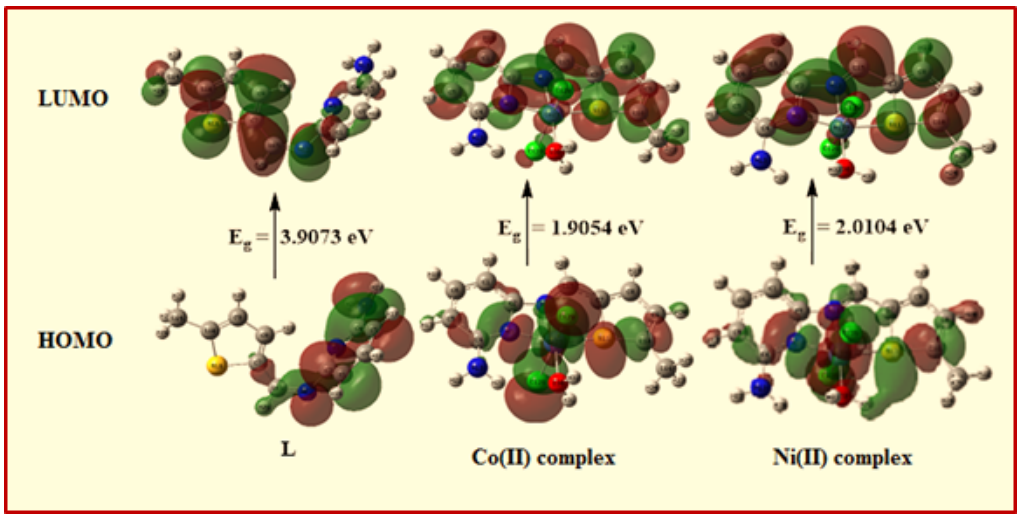

Figure 12

HOMO and LUMO charge density maps of ligand, [CoL(H_2O)Cl_2] and [NiL(H_2O)Cl_2].

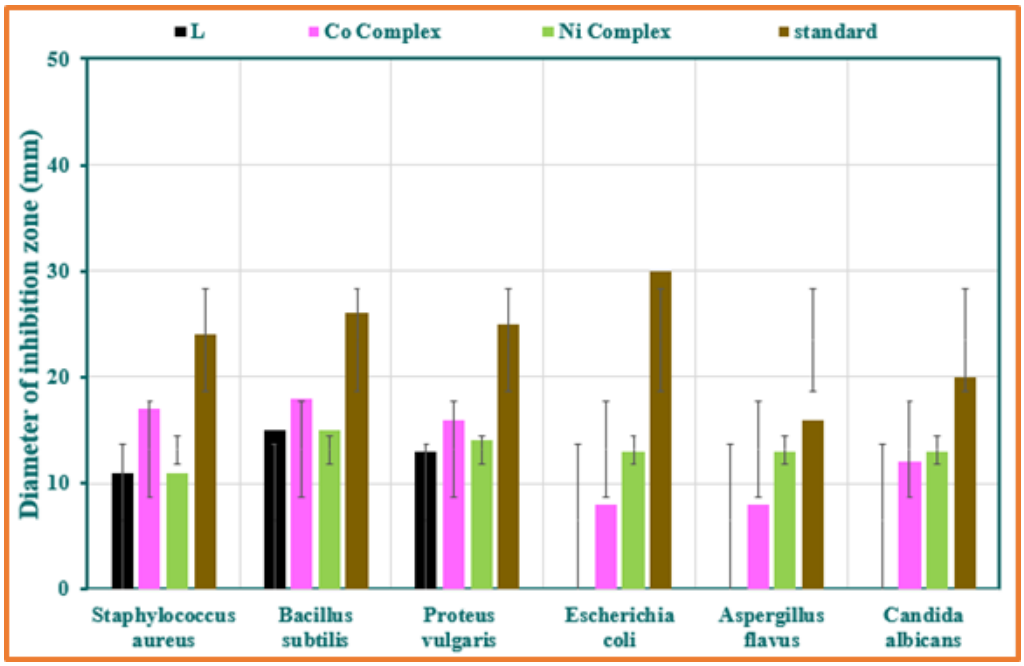

Figure 13

Effect of antimicrobial activity of the ligand and its metal complexes.

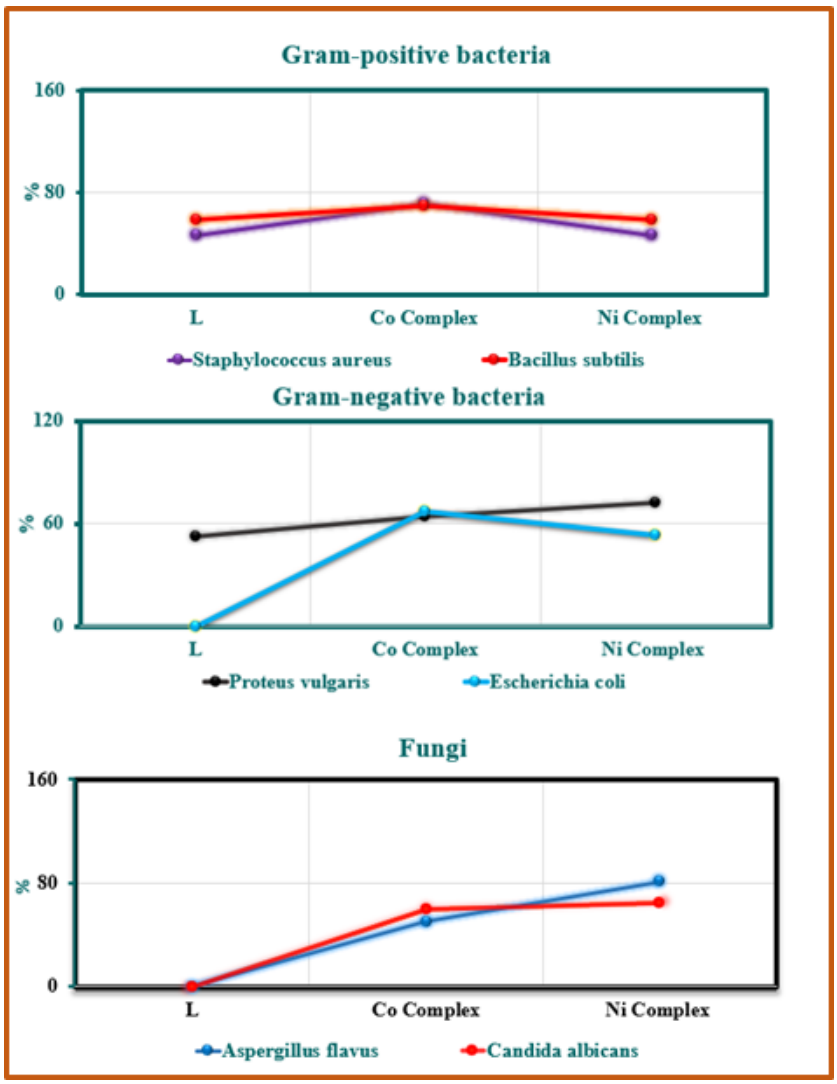

Figure 14

Activity index of the Schiff base ligand and its complexes.

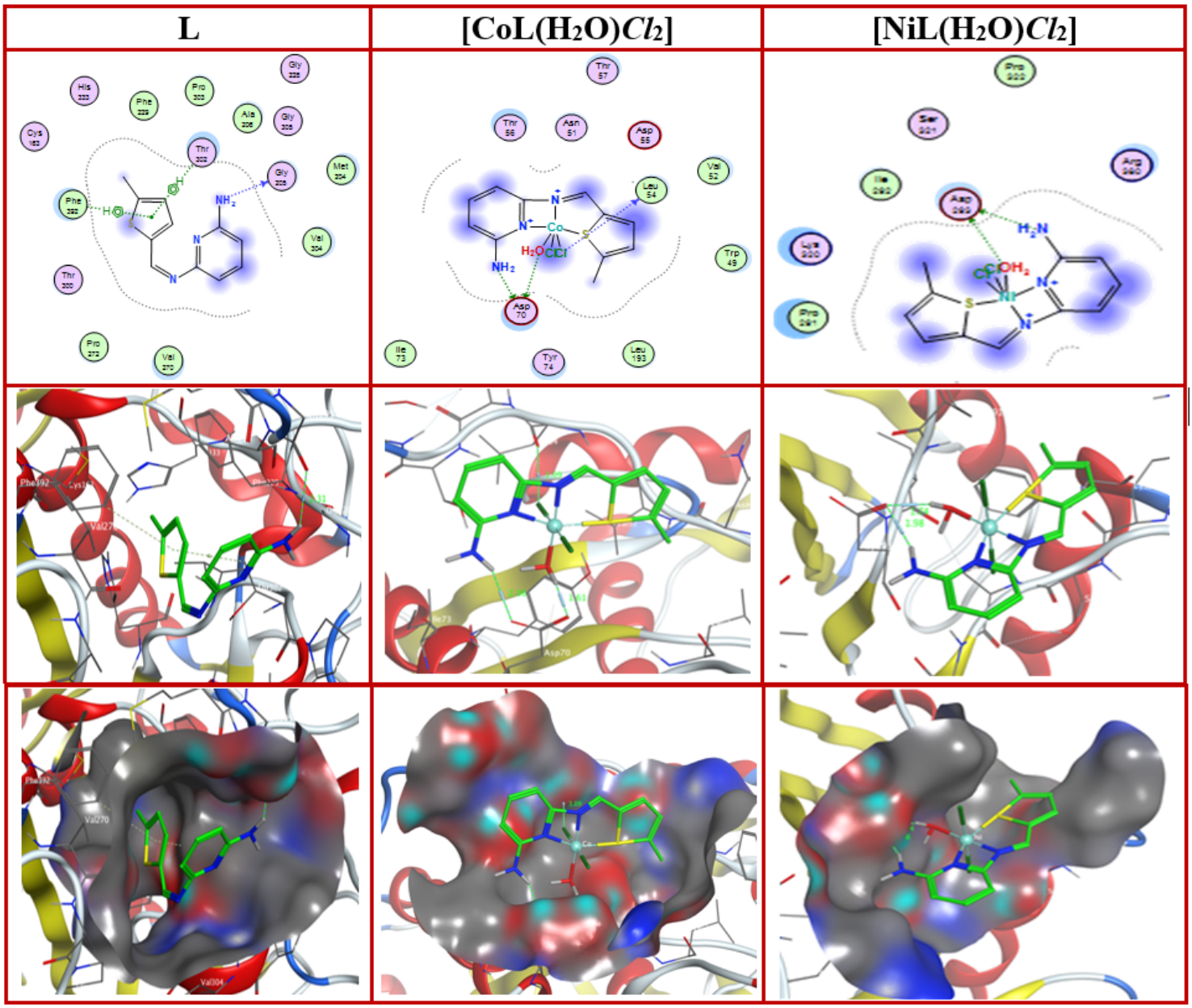

Figure 15

2D and 3D plots of the interactions between L, [CoL(H_2O)Cl_2] and [NiL(H_2O)Cl_2] with the active site of Escherichia coli (gram –ve bacteria) (PDB ID: 1fj4). Hydrophobic interactions with amino acid residues are shown with dotted curves.

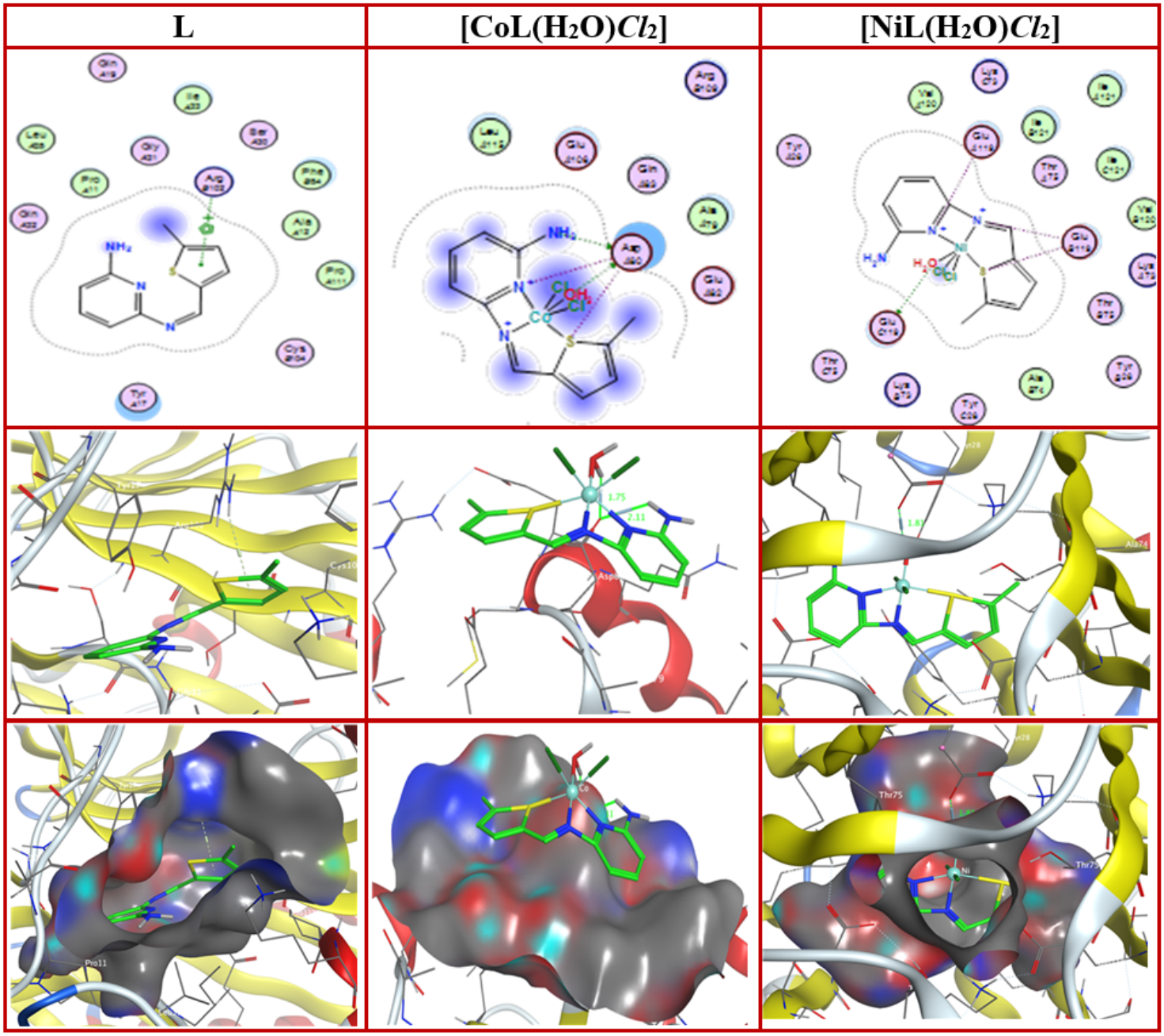

Figure 16

2D and 3D plots of the interactions between L, $[CoL(H_2O)Cl_2]$ and $[NiL(H_2O)Cl_2]$ with the active site of the receptor of Bacillus subtilis (PDB ID: 1QD9). Hydrophobic interactions with amino acid residues are shown with dotted curves.